RGNZ/MGPB

Preliminary Petromagnetic Study of 1849, 1926, 1963, 1968 and 1974 Surface Lavas from Batur Volcano, Bali, Indonesia: Insight on the Magmatic Process of Source and Rock Magnetic Nature

Rudarsko-geološko-naftni zbornik
(The Mining-Geology-Petroleum Engineering Bulletin)
UDC: 551.21
DOI: 10.17794/rgn.2023.1.3

Preliminary communication

Putu Billy Suryanata[1,3], Satria Bijaksana[1], Mirzam Abdurrachman[2], Darharta Dahrin[1], Aditya Pratama[2,3], Nuresi Rantri Desi Wulan Ndari[1], Silvia Jannatul Fajar[1]

[1] *Faculty of Mining and Petroleum Engineering, Institut Teknologi Bandung, Jalan Ganesa 10, Bandung 40132, Indonesia.*
[2] *Faculty of Earth Sciences and Technology, Institut Teknologi Bandung, Jalan Ganesa 10, Bandung 40132, Indonesia.*
[3] *Research Centre for Geological Disaster, National Research, and Innovation Agency (BRIN), Bandung 40135, Indonesia*

Abstract

Geochemical and petrographic characterizations were carried out on five episodic effusive eruptions from Batur Volcano on the Island of Bali, Indonesia, and revealed that these lavas are basaltic to andesitic in composition. Various micro-textures were identified, reflecting pre-eruptive magmatic processes, magma mixing, and adiabatic decompression. Apart from XRF analyses, the five lava flows (L849, L926, L963, L968 and L974) were subjected to magnetic analyses in the form of magnetic susceptibility and magnetic hysteresis measurements. The presence of cyclicity in the magmatic process is suggested by the variation of micro-texture types, CaO content, and magnetic susceptibility values. Two possible models of this cyclicity are presented. In the first model, cyclicity is driven by the variation of influx from the lower magma chamber that affects the interaction of magma with the surrounding rocks. In the second model, cyclicity is affected by the appearance of a new magmatic vent, which causes intense interaction with surrounding rocks. This study infers that combined micro-texture, composition, and magnetic susceptibility analyses might provide insight into the cyclicity of lava episodes observed in active volcanos such as Batur.

Keywords:
Batur Volcano; magmatism; petrogenesis; rock magnetism; Bali

1. Introduction

Batur Volcano on the island of Bali, Indonesia is a stratovolcano with two main calderas composed of well-dated volcanic products, including successive lava flows (**Wheller and Varne, 1986**). The calderas were formed in six stages and produced volcanic products (lava, pyroclastic and ignimbrite) ranging from basaltic to rhyolitic in composition (**Reubi and Nicholls, 2005**). Most of the lava flows of Batur Volcano are blocky, ʻAʻā type lava located in the middle of the summit caldera (**Wheller and Varne, 1986; Reubi and Nicholls, 2004; Reubi and Nicholls, 2005**) and have been mapped by **Sutawidjaja et al. (1992)**. Well mapped and dated lava from Batur Volcano can be an interesting substance to learn more about magmatism processes. The process in the magma chamber comprises activities such as magma crystallization, injections of a new magma batch from a deeper source, mixing with pre-existing magma, and magma transport to shallower depths or to the surface, which leads to an eruption (**Nurfiani et al., 2021**). Understanding the processes in the magma chamber can assist in the interpretation of past and current eruption behaviour, allowing for better hazard assessments and eruption forecasting. One way is to find out whether there is a cycle of eruptions in the volcano (**Sahoo et al., 2022**). In an island arc like Java or Bali, another important aspect that needs to be considered is the interaction between magma and carbonate basement rock, as such an interaction might affect the geochemistry of the lava as well as the eruption mechanism (**Deegan et al., 2010**).

An earlier study of Batur Volcano effusive products by **Geiger et al. (2018)** focused only on two lava flows formed in 1963 and 1974. The authors used a combination of petrographic and thermobarometric methods to suggest that the lavas were the products of a multi-level magmatic plumbing system. This study concluded that there are two magma chambers at two different depths beneath Batur Volcano. That study, using thermobarometric analyses, pointed out that the 1963 lava came from two different mixed magma chambers, one of which is located at a depth of 12-18 km and another chamber located at a depth of 2-4 km. The 1974 lava also ascended from two different mixed magma chambers which are located at a depth of 15-19 km and 3-5 km respectively (**Geiger et al., 2018**). The existence of such a multi-level plumbing system in Batur Volcano

Corresponding author: Satria Bijaksana
e-mail address: satria@itb.ac.id

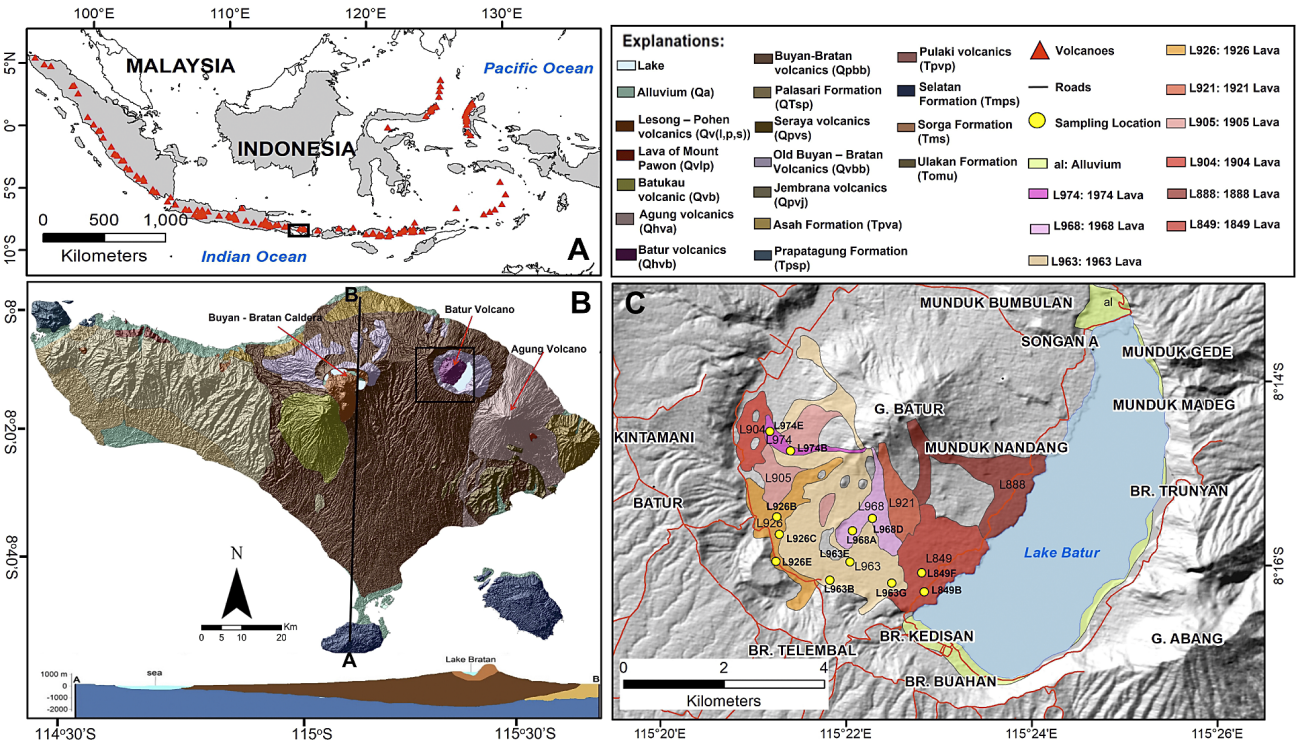

Figure 1: (A) Map of volcanoes in Indonesia, (B) Geological Map of Bali, including the cross-section of the island (modified after **Purbo-Hadiwidjojo et al., 1998; Purnomo and Pichler, 2015**), and (C) Geological Map of Batur Volcano, including the lavas of Batur Volcano and sampling locations (modified after **Sutawidjaja et al., 1992**).

and the nearby Agung Volcano was also suggested by **Syahbana et al. (2019)** using different approaches. These authors used a combination of seismicity, remote sensing, and geochemistry to model the magma chamber under the Batur and Agung volcanos and proposed the existence of crystallized remains of the Batur Caldera reservoir that is traversed by magma vents to reach the surface. Using a pre-eruptive seismic swarm at Agung Volcano, **Albino et al. (2019)** identified dyke intrusions between Batur and Agung volcanoes, while the deeper chamber, which is closer to Moho, is termed the lower crustal magma source. In this study, we present a combination of petrographic, geochemical, and rock magnetic analyses on five different lava flows (1849, 1926, 1963, 1968, and 1974) from Batur Volcano to further our understanding of its magmatic processes and the effusive eruptive cycle. Such knowledge is crucial for monitoring and reducing volcanic hazard in nations with a lot of active volcanoes, for example the United States of America, Russia, Indonesia, Japan, Iceland, and many more nations.

2. Material and Methods

Rock samples were collected from five lava flow units, which were classified according to the year the lava was formed: L849, L926, L963, L968, and L974. In total 12 samples were taken for further measurements and analysis. Two samples from each of L849, L968 and L974 and three samples from each of L926 and L963 (see **Figure 1**). The samples were collected from the surface of the lava (see **Figure 2C**). The sample numbers reflect their eruptive episodes (i.e. L926B, C, and E, are the three samples collected from the lava that erupted in 1926). Sample locations were chosen based on the conditions of the lavas as well as their availability, as some of the lava surfaces have been converted to agricultural and residential areas (for instance, L904, L905 and L888). Some lavas are also difficult to reach due to cover and harsh terrain (L921).

Magnetic susceptibility parameters were measured with mass-specific magnetic susceptibility at low frequency, 470 Hz and termed χ_{LF}, as well as at high frequency, 4700 Hz and termed χ_{HF}. The third parameter is the frequency-dependent magnetic susceptibility (χ_{FD}) and is calculated as $(\chi_{LF} - \chi_{HF})/\chi_{LF}$. The χ_{LF} and χ_{HF} parameters were measured using a Bartington MS2B and MS3 magnetic susceptibility system (Bartington Instrument Ltd., Witney, UK at the Laboratory for Characterization and Modelling of Rock Physical Properties, Bandung Institute of Technology). All measurements were performed using the instrument and steps previously described in **Santoso et al. (2017)**. We then determine which representative sample to utilize to calculate the hysteresis parameter based on the difference in magnetic susceptibility values between samples in the same lava flow. When there is a considerable difference in magnetic susceptibility across samples, the hysteresis parameter measurement is performed on more than one sample. Hysteresis parameters were measured using a

vibrating sample magnetometer (VSM 1.2 H/CT/HT by Oxford Instrument, Oxfordshire, UK) at BRIN (*Badan Riset dan Inovasi Nasional* or the National Research and Innovation Agency) in Serpong, Banten, Indonesia. Each hysteresis parameter was saturated with magnetization (*Ms*), saturation remanence (M_{rs}), coercivity (H_c), and coercivity of remanence (H_{cr}). These hysteresis parameters are then determined and plotted on a Day's plot (**Day et al., 1977**; **Figure 3A**), which can be used to recognize the type of magnetic domain. In addition, plots of squareness (M_{rs}/M_s) with coercivity (H_c) (**Wang and Van der Voo, 2004**; **Figure 3B**) were also made to qualitatively estimate magnetic mineral types.

The petrographic examination, done at the Petrology Laboratory, Institut Teknologi Bandung, was used to determine mineral compositions and to determine the micro-texture of plagioclase in the samples. Micro-texture in plagioclase can be used to interpret what processes occur in the magma chamber (**Renjith, 2014**). Geochemical analyses were done by XRF (X-ray fluorescence) at the Institut Teknologi Bandung. XRF measurements were carried out for nine samples in total, selected as representative samples based on the results of magnetic susceptibility measurements.

Figure 2: Sampling location for lava sample L849 F in the surface of lava flow at the Batur Volcano area. The red dashed squares indicate sampling locations.

3. Results

Summarized results of magnetic susceptibility measurements for all samples are shown in **Table 1**. Although the values of χ_{LF} and χ_{FD} are quite variable within a particular lava flow, their average values reveal consistent differences between lavas. Thus, the average values of samples for the 1849 lava are significantly lower than those of the other four lavas, while lava samples from 1926 and 1963 have significantly higher average values. In each lava flow, the magnetic susceptibility values differ significantly between the samples. For instance, in L849 lava, samples collected from the middle of the lava have higher magnetic susceptibility compared to those collected from the surface. The situation is completely opposite in the L926 lava (see **Table 1**). The values of χ_{FD} (%) show less diversity, ranging between 1.78 and 3.25%. Low average values of less than 2% (as detected in the 1926 and 1974 lava samples) infer that these samples contain predominantly a mixture of SD (single domain), PSD (pseudo-single domain) and MD (multi domain) grains (**Dearing, 1999**). The presence of SP (superparamagnetic) grains is detected only in the 1849, 1963, and 1968 samples where their average χ_{FD} (%) values are greater than 2%.

The plot of hysteresis parameters in a modified Day's plot as suggested by **Dunlop (2002)** (see **Figure 3A**). Each lava flow is represented by a different number of samples based on the variety of magnetic susceptibility values. The L849 lava samples have a relatively similar magnetic susceptibility and are represented by only one sample for the hysteresis parameter. Meanwhile, the L926 lava samples with diverse values of magnetic susceptibility are represented by two samples for hysteresis parameters. It is evident from **Figure 3A** that the predominant magnetic domain in all samples from Mount Batur is PSD. Each lava flow also shows its unique clustering pattern. Samples from the L968 lava tend to be clustered together, inferring similar magnetic characteristics, while samples from the L926 lava tend to be scattered inferring diverse magnetic characteristics. The hysteresis parameters of one sample from L926 lava falls in the region that is associated with SD/SP domain. The diverse magnetic characteristics of samples from the L926 lava might be associated with their diversity in geochemistry (see **Table 2**).

Table 1: Magnetic susceptibility values of the surface lava samples at Batur Volcano

Sample	χ_{LF} (10^{-8} m^3/kg)	χ_{FD} (%)
L849B	542.22	3.14
L849F	412.86	2.17
Average	477.54 ± 64.68	2.66 ± 0.49
L926B	2235.8	1.8
L926C	1147.02	1.87
L926E	1401.55	1.46
Average	1594.79 ± 465.02	1.71 ± 0.18
L963B	1927.89	3.83
L963E	1188.15	2.32
L963G	1093.14	3.26
Average	1403.06 ± 373.13	3.14 ± 0.62
L968A	858.74	2.7
L968D	826.11	3.07
Average	842.43 ± 16.32	2.89 ± 0.19
L974B	533.38	1.76
L974E	766.96	2.26
Average	650.17 ± 116.79	2.01 ± 0.25

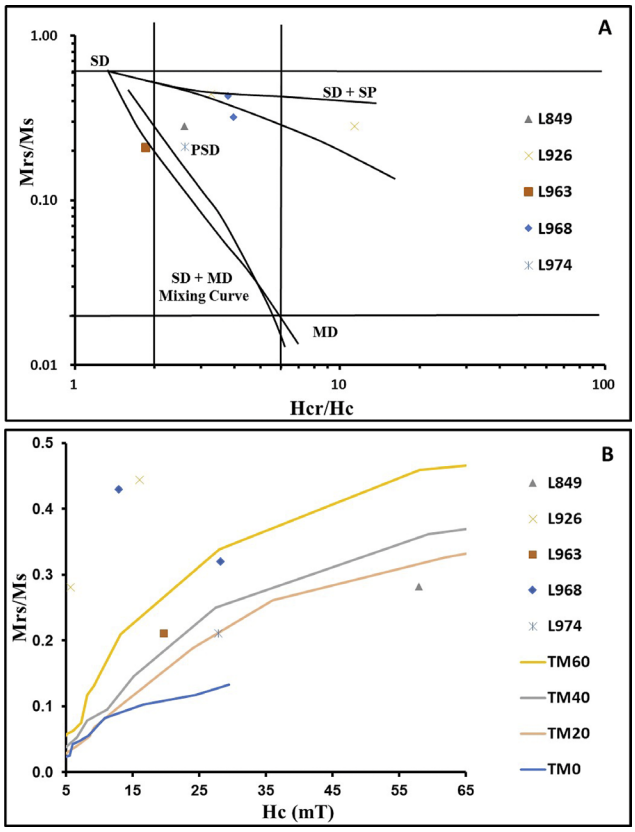

Figure 3: (A) The modified Day's plot proposed by **Dunlop (2002)** showing the magnetic particles from the sample are dominated by PSD grain and (B) the squareness (M_{rs}/M_s) plots vs Applied Magnetic Field (H_c) proposed by **Wang and Van der Voo (2004)** to estimate the type of magnetic mineral. Other symbols represent the following: SD for Single Domain, PSD for Pseudo Single Domain, MD for Multi Domain, SP for Super Paramagnetic, TM0, TM20, TM40, TM60 for a content of 0%, 20%, 40%, and 60% of the maximum total Ti contained in a magnetic mineral respectively.

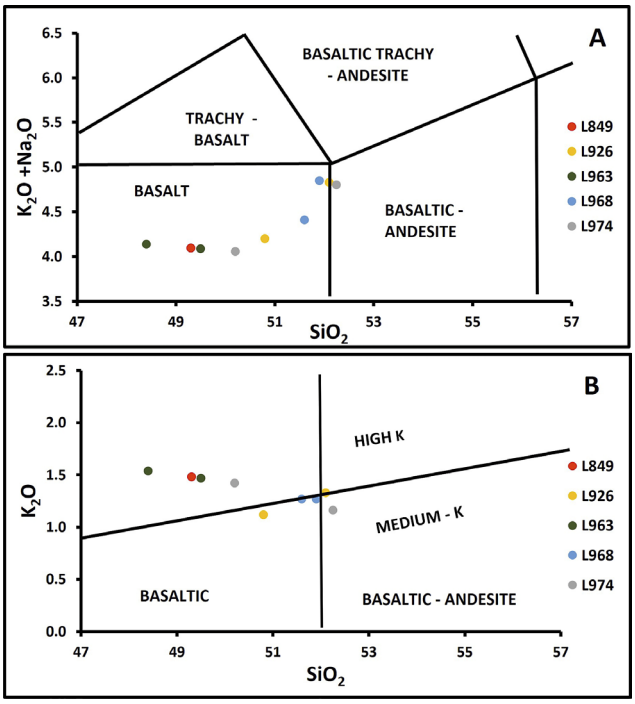

Figure 4: (A) Plot of SiO_2 vs NaO_2 + K_2O content of lava samples to represent each Batur Volcano surface lava flow in the Total Alkali Silica Diagram (modified after **Le Bas et al., 1986**) indicates that all the samples have basaltic to basaltic-andesite composition. (B) Plot of SiO_2 content against K_2O content of lava samples to represent each Batur Volcano lava flow in the Peccerillo and Taylor diagram (modified after **Peccerillo and Taylor, 1976**) indicates that sample from Batur Volcano classify to 2 different magma sources which have high and medium potassium content.

Hysteresis parameters can also be presented in the form of different curves, namely squareness (M_{rs}/M_s) vs H_c (see **Figure 3B**). This ratio can be used to estimate the type of magnetic mineral contained in the sample.

Table 2: Major element compositions (in weight %) of Batur surface lava samples

Sample	L849	L926			L963			L968			L974		
	F	B	E	Average	B	G	Average	A	D	Average	B	E	Average
SiO_2	49.30	52.10	50.80	51.45 ± 0.65	49.50	48.40	48.95 ± 0.55	51.60	51.90	51.75 ± 0.15	52.25	50.20	51.22 ± 1.02
Al_2O_3	17.65	21.70	21.20	21.45 ± 0.25	17.70	17.41	17.55 ± 0.14	21.70	21.70	21.7 ± 0.00	18.88	17.88	18.38 ± 0.50
Fe_2O_3	9.75	8.03	9.50	8.77 ± 0.74	9.64	10.23	9.94 ± 0.29	8.60	8.43	8.52 ± 0.09	9.25	9.27	9.26 ± 0.01
MgO	5.37	1.44	2.46	1.95 ± 0.51	5.28	5.79	5.53 ± 0.26	1.75	1.53	1.64 ± 0.11	3.99	4.95	4.47 ± 0.48
CaO	9.63	10.10	10.10	10.10 ± 0.00	9.92	10.10	10.01 ± 0.09	10.20	10.00	10.10 ± 0.10	8.89	9.43	9.16 ± 0.27
Na_2O	2.62	3.50	3.08	3.29 ± 0.21	2.62	2.60	2.61 ± 0.01	3.14	3.58	3.36 ± 0.22	3.64	2.63	3.14 ± 0.50
K_2O	1.48	1.33	1.12	1.23 ± 0.11	1.47	1.54	1.50 ± 0.04	1.27	1.27	1.27 ± 0.00	1.16	1.42	1.29 ± 0.13
TiO_2	1.74	0.81	0.91	0.86 ± 0.05	1.26	1.60	1.43 ± 0.17	0.88	0.84	0.86 ± 0.02	1.04	1.54	1.29 ± 0.025
P_2O_5	0.25	1.33	0.20	0.76 ± 0.57	0.25	0.24	0.25 ± 0.01	0.21	0.19	0.20 ± 0.01	0.17	0.27	0.22 ± 0.05
MnO	0.43	0.17	0.18	0.17 ± 0.01	0.41	0.50	0.45 ± 0.05	0.17	0.18	0.17 ± 0.01	0.18	0.53	0.35 ± 0.17
Total	98.21	100.52	99.55	100.03 ± 0.49	98.05	98.41	98.23 ± 0.18	99.52	99.62	99.57 ± 0.05	99.45	98.12	98.79 ± 0.66
LOI	0.35	-	0.14	-	-	0.32	-	-0.12	-	-	-	-0.28	-

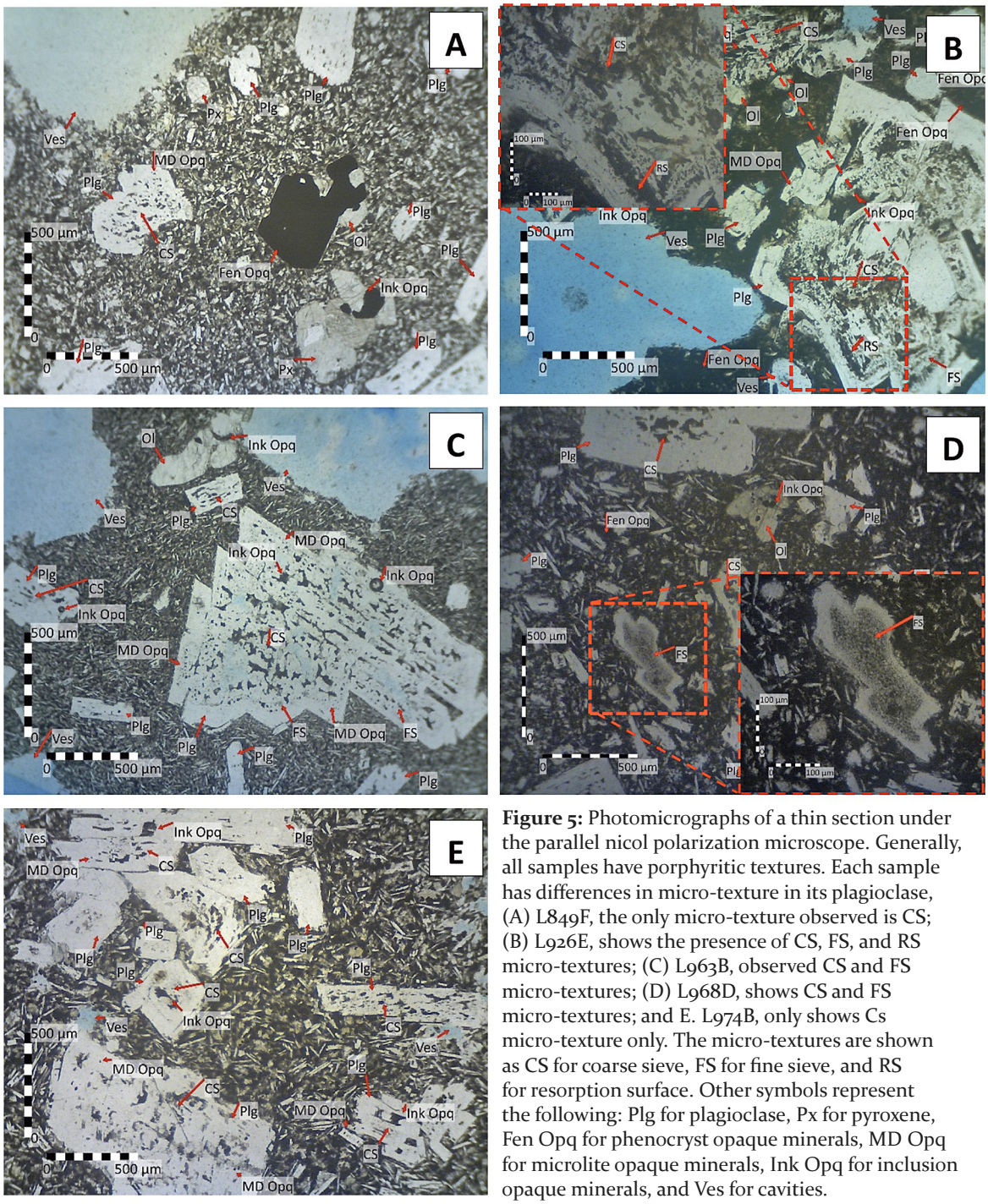

Figure 5: Photomicrographs of a thin section under the parallel nicol polarization microscope. Generally, all samples have porphyritic textures. Each sample has differences in micro-texture in its plagioclase, (A) L849F, the only micro-texture observed is CS; (B) L926E, shows the presence of CS, FS, and RS micro-textures; (C) L963B, observed CS and FS micro-textures; (D) L968D, shows CS and FS micro-textures; and E. L974B, only shows Cs micro-texture only. The micro-textures are shown as CS for coarse sieve, FS for fine sieve, and RS for resorption surface. Other symbols represent the following: Plg for plagioclase, Px for pyroxene, Fen Opq for phenocryst opaque minerals, MD Opq for microlite opaque minerals, Ink Opq for inclusion opaque minerals, and Ves for cavities.

The hysteresis parameters obtained in this study were compared with the trend of data from several types of magnetic minerals that have different percentages of Ti content from titanomagnetite obtained from **Wang and Van der Voo (2004)**. For example, the TM20 line indicates a content of 0.2 or 20% of the maximum total Ti contained in a magnetic mineral. The types of magnetic minerals in samples from lava flows L849 and L974 have magnetic mineral types between the TM20 and TM0 lines. The flow of L926, L963, and L968 is above the TM40 line. From this case, we can see that there are two groups of samples based on the type of magnetic mineral. Based on **Table 2**, the L849 and L974 lava group has a higher Ti content compared to the L926, L963, and L968 lava group despite its low TM number. This is probably due to the fact that not all Ti would form titanomagnetite. Titanomagnetite mineralogy is rather complicated as there are variations due to variables such as grain size, composition, and maghemitization (**Zhou et al., 2000**).

Whole-rock compositional data is shown in **Table 2**. The results are plotted in **Figure 4A** on a total alkali-silica diagram (TAS) after **Le Bas et al., 1986** that shows the types of rock samples are dominantly basalt. The

SiO_2 vs K_2O diagram (**Peccerillo and Taylor, 1976; Figure 4B)** suggests that the samples from 1926 and 1968 could be classified as medium potassium content, whereas most samples from 1849, 1963, and 1974 have high potassium content.

Photomicrographs of representative samples from each lava flow are shown in **Figure 5**. All samples have porphyritic textures. Generally, they include plagioclase, pyroxene, opaque minerals, and olivine minerals as phenocrysts. The opaque minerals, black in both cross nicol and parallel nicol modes, are responsible for the magnetic properties of rocks (**Pratama et al., 2018**). The presence of three different micro-textures, namely CS (coarse sieve), FS (fine sieve), and RS (resorption surface) micro-textures also seen in the thin section of representative samples (see **Figure 5**). CS and FS are the glass inclusions in plagioclase, but they differed in size. RS are the horizons, like an unconformity surface marking a boundary between two textural domains or growth zones. CS micro-texture was observed in all lavas (see **Figure 5A, B, C, D, E**), while FS micro-texture was observed in the 1926, 1963, and 1968 lavas (see **Figure 5B, C, D**). The RS micro-texture was observed only in the 1926 lava (see **Figure 5B**).

4. Discussion

Rock samples were taken from five lava flow units, which were differentiated based on the year the lava was formed, namely L849, L926, L963, L968, and L974. Based on geochemical and petrographic analysis from measurement data and observations of outcrops and hand specimens, all the samples are determined as basaltic lavas. Petrogenetically, all samples have similarities in texture and characteristics, probably due to similar mineral forming processes in the surface. The variability of geochemical results, however, infers that the lava products from Batur Volcano are not homogeneous. Batur and the nearby Agung Volcano have been identified to have multi-level magma plumbing (**Geiger et al., 2018**). Observations in this study identify CS micro-textures inferring dissolution of varying rates of the adiabatic decompression of H_2O-undersaturated magma. Also, there are FS micro-textures which indicate partial dissolution due to reacting with more calcium-rich melts (**Renjith, 2014).**

The presence of CS micro-textures in plagioclase indicates that the lava products that were analysed in this study originated from magma mixing processes (**Renjith, 2014**). The FS micro-texture (which was only found in L926, L963 and L968 lava samples) infers generally more basaltic magma as it is also indicated by higher CaO content (see **Figure 6A**). Apart from the presence of FS micro-texture and high CaO content, the lavas L926, L963, and L968 have higher magnetic susceptibility. L849 and L974 lavas lack the FS micro-textures and also have lower magnetic susceptibility values in regard

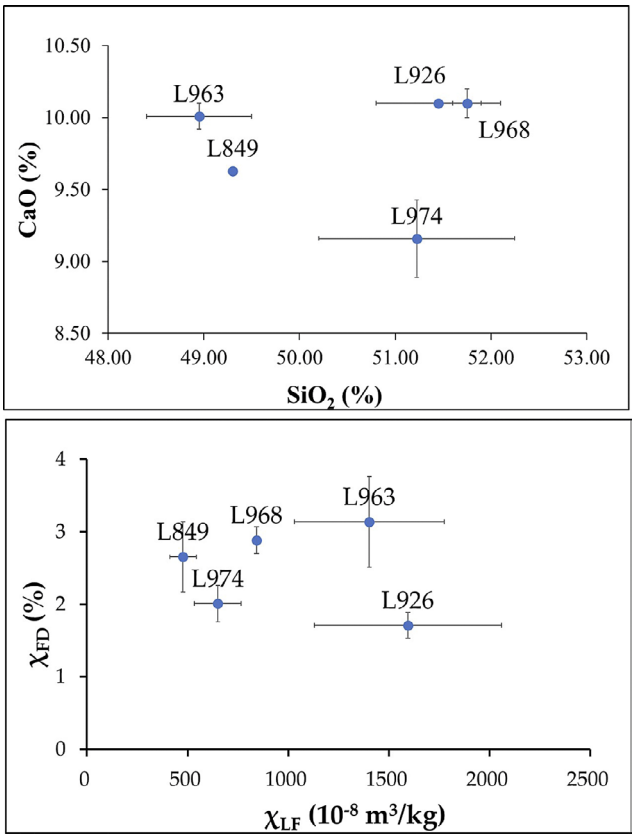

Figure 6: (A) Plot of average percentages of SiO_2 and CaO for each surface lava samples. (B) Plots of average χ_{LF} and χ_{FD} (%) of each flow located on the surface of the lava.

to L926, L963, and L968 lavas (see **Figure 6B**). This infers that the L849 and L974 lava group have different characteristics than the L926, L963, and L968 lava group. The variation of FS presence, CaO content and magnetic susceptibility values indicate cyclicity.

Unlike other lavas, the L926 lava contain RS micro-texture in its plagioclase. The RS micro-texture indicates intense and prolonged dissolution while reacting with more primitive magma (**Renjith, 2014**). Since the results of geochemical measurements of L926 lava do not confirm any reaction with more primitive magmas, the RS micro-texture might reflect an interaction between magma chambers or magma mixing. If so, then the intensity of such an interaction might drive the cyclicity of magmatic processes. On the other hand, the interaction between magma and the surrounding rocks is supported by other evidence. Such an interaction between magma and surrounding rocks might alter the chemistry without producing micro-textures. Unlike that of other caldera lakes, the magmatic water of Lake Batur, tend to be basic rather than acidic with a pH level of 9.4 ± 0.2 (**Sukmawantara et al., 2021**). This alkalinity is probably due to interactions with limestones or carbonate-rich rocks. Although there is no sufficient information regarding the surrounding rocks that interact with the magma, there are two possibilities. The first possibility is the crystallized remains of the Batur caldera reservoir at depth of

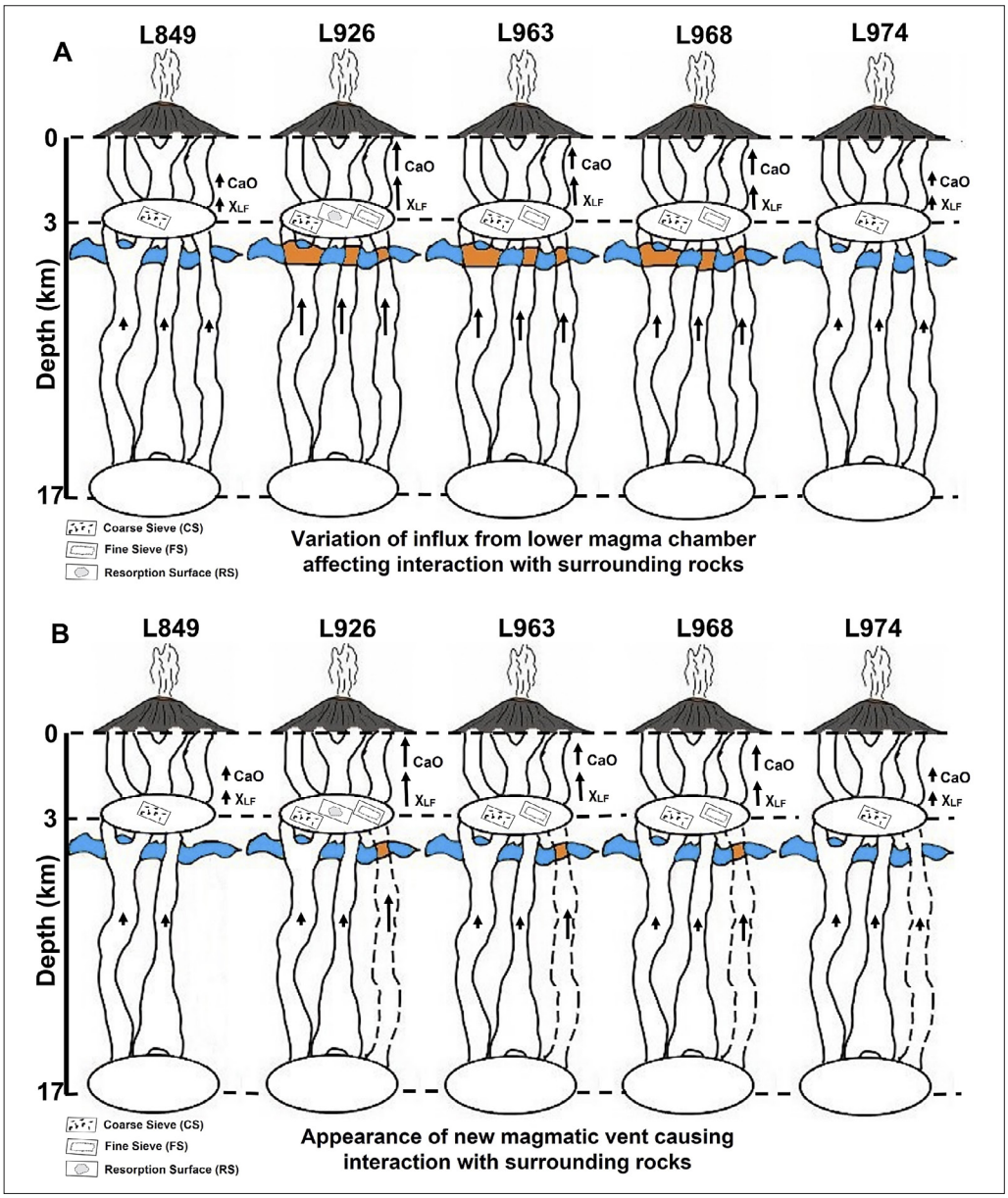

Figure 7: Models of interaction between magma and surrounding rocks. The presence of micro-textures (CS, FS, RS) depend on the intensity of the interaction between magma and surrounding rocks. (A) The first model based on the variation of influx from the lower magma chamber that affects the interaction with surrounding rocks. (B) The second model based on the appearance of a new magmatic vent (since 1926), causing intense interaction with surrounding rocks. The depth of the magma chamber under Batur volcano is based on **Geiger et al. (2018)**. The blue bodies are the crystallized remains of the Batur Caldera reservoir (**Syahbana et al., 2019**) or carbonate wall rock. The orange bodies indicate the interaction between surrounding rocks and magma influx. The dotted line shows the new magmatic vent. The relative amount of CaO content, magnetic susceptibility value, and magma influx from the lower magma chamber are indicated by the length of the bold arrows.

about 5 km deduced by **Syahbana et al. (2019)**. The lithology of the reservoir is unknown. The second possibility is the limestones or carbonate-rich rocks from the Selatan and Prapatagung formations, like that found in the island of Nusa Penida or in the Nusa Dua Peninsula (**Figure 1; Purbo-Hadiwidjojo et al., 1998**). It has also been described by **Purnomo and Pichler (2015)** that the possibility of carbonate-rich rocks from the Selatan and the Prapatagung formations are covered by a quarter volcanic formation in the central part of the island of Bali (see **Figure 1**). An interaction between magma and the surrounding rocks containing carbonates might increase the CaO content but might not affect SiO_2, Al_2O_3 and MgO. An experimental study by **Deegan et al. (2010)** on lava and carbonate rock on Merapi Volcano in Central Java, showed that such an interaction might in-

crease the CaO content of the lava. The study by **Deegan et al. (2010)** also pointed out that carbonate assimilation could be identified by physical mingling between the contaminated and unaffected melt domains as well as chemical mixing between melts. These two processes might in turn affect the magnetic mineralogy of the lava, creating more magnetic minerals. This hypothesis is currently being tested by using magnetic mineralogical analysis on the lava sample of Batur Volcano. Compared to that of L926, the lavas of L963 and L968 have lower Ca content and lower magnetic susceptibility values, inferring the interaction between magma and the surrounding rocks in these lavas was less intense than that of L926.

So, what would be the main cause(s) affecting the intensity of interaction between magma and the surrounding rocks? Here, two models on the intensity of magma interactions with the surrounding rocks are presented. In the first model (see **Figure 7A**), the intensity of interaction depends on the influx from lower magma chamber. In L849, the influx from the lower chamber is relatively small so that intensity of interaction is also minimum. This was represented by the presence of CS micro-textures, low CaO content and low magnetic susceptibility values. In L926, the influx from the lower chamber is relatively intense causing strong interaction between magma and the surrounding rocks. This strong interaction is reflected in the presence of CS, FS, and RS micro-textures, high CaO content, and high magnetic susceptibility values. In L963 and L968, the influx from the lower chamber has been decreased reducing the intensity of interaction between magma and the surrounding rocks. This is reflected in the absence of RS micro-textures and reduced CaO content as well as lower magnetic susceptibility values. In L974, the influx from the lower chamber is returning to the same level as that in L849, reflected in the presence of CS micro-textures only with low CaO content and low magnetic susceptibility values.

In the second model (see **Figure 7B**), the high intensity of magma interaction with the surrounding rocks is attributed to the appearance of a new magmatic vent. In L849, there is no new magmatic vent so that the intensity of interaction is minimal. In L926, a new magmatic vent appears to be intensifying the interaction between magma and the surrounding rocks reflected in the presence of CS, FS, and RS micro-textures, high CaO content, and high magnetic susceptibility values. Young plumbing systems are relatively cool and contain large amounts of wall rock contaminants, and ascending magmas undergo contamination as well as concurrent crystallization and fractionation (**Myers et al., 1985**). In L963 and L968, the intensity of interaction between magma and the surrounding rocks decreased with time, heat and mass transfer between ascending magmas and wall rock produce thermal and chemical boundary layers that insulate subsequent magmas (**Myers et al., 1985**). With this reduced intensity, the L963 and L968 lavas do not contain RS micro-textures while their CaO content and magnetic susceptibility values are lower than that of L926. In L974, the heat and mass transfer between ascending magma and the surrounding rocks have returned to the similar state as in L849.

These two proposed models are speculative and certainly require further analyses to confirm their validity. In Batur Volcano, the presence of underneath surrounding rocks might be validated or confirmed from geophysics surveys using gravity and magnetic methods. The two proposed models could also be tested in other volcanic systems that have well-recorded lavas from multiple eruptions. Within Indonesia, Krakatoa and Ijen volcanic complexes are suitable candidates for testing the models.

5. Conclusion

This preliminary petromagnetic study on five lava flows (L849, L926, L963, L968, and L974) from Batur Volcano, on the island of Bali, Indonesia, shows that the lava flows could be distinguished into two different groups based on their types of micro-textures, CaO content, and magnetic susceptibility values. The first group (L849 and L974) are characterized by the presence of only CS micro-textures, low CaO content, and low magnetic susceptibility. In contrast, the second group (L926, L963, and L968) are characterized by the presence of CS and FS micro-textures, high CaO content, and high magnetic susceptibility value. This grouping and the presence of RS micro-texture in L926 suggest that there was a cyclicity in the magmatic processes. To explain the cyclicity, two possible models for interaction between magma and the surrounding rocks are presented. In the first model, variations in influx from the lower magma chamber affect the intensity of interaction between magma and the surrounding rocks. The intensity of this interaction, in turn, controls the presence of FS and RS micro-textures, the CaO content, and magnetic susceptibility value. In the second model, the cyclicity and the intensity of such interactions are driven by the presence of a new magmatic vent. The two models still require validation from similar studies in other volcanic complexes. The cyclicity of magmatic process is invaluable knowledge that is crucial for monitoring and reducing volcanic hazards.

Acknowledgement

The permission to conduct field research at Batur Volcano was given by the BKSDA (*Balai Konservasi Sumber Daya Alam* or the Natural Resource Conservation Centre) of Bali, Indonesia. Two anonymous reviewers are thanked for their constructive comments on the earlier version of the manuscript. Financial support for this research was provided by the Ministry of Education, Culture, Research, and Technology of the Republic of

Indonesia through the basic research scheme (*Hibah Penelitian Dasar*).

6. References

Albino, F., Biggs, J., Syahbana, D.K. (2019): Dyke intrusion between neighbouring arc volcanoes responsible for 2017 pre-eruptive seismic swarm at Agung. Nature Communication, 10, 748. doi: 10.1038/s41467-019-08564-9.

Day, R., Fuller, M., dan Schmidt, V. (1977): Hysteresis Properties of Titanomagnetites: Grain-size and Compositional Dependence, Physics of the Earth, and Planetary Interiors, 13, 260-267. doi: 10.1016/0031-9201(77)90108-X.

Dearing, J. A. (1999): Environmental Magnetic Susceptibility using the Bartington MS2 system. British Library Cataloguing in Publication Data, London.

Deegan, F. M., Troll1, V. R., Freda, C., Misiti, V., Chadwick, J. P., Mcleod, C. L, Davidson, J. P. (2010): Magma - Carbonate Interaction Processes and Associated CO2 Release at Merapi Volcano, Indonesia: Insights from Experimental Petrology. Journal of Petrology, 51(5), 1027 – 1051. doi: 10.1093/petrology/egq010.

Dunlop, D. J. (2002): Theory and application of the Day plot (Mrs/Ms versus Hcr/Hc) 2. Application to data for rocks, sediments, and soils. Journal of Geophysical Research, 107, B3. doi: 10.1029/2001JB000487.

Geiger, H., Troll, V., Jolis, E., Deegan, F., Harris, C., Hilton, D., Freda, C. (2018): Multi – level magma plumbing at Agung and Batur volcanoes increases risk of hazardous eruptions, Science Report, 8, 10547. doi:10.1038/s41598-018-28125-2

Le Bas, M. J., Le Maitre, R., Streckeisen A., Zanettin B. (1986): A Chemical Classification of Volcanic Rocks Based on the Total Alkali – Silica Diagram. Journal of Petrology, 27, 745 – 750. doi: 10.1093/petrology/27.3.745.

Myers, J.D., Marsh, B.D. & Sinha, A.K. (1985): Strontium isotopic and selected trace element variations between two Aleutian volcanic centers (Adak and Atka): implications for the development of arc volcanic plumbing systems. Contribution to Mineralogy and Petrology, 91, 221–234. doi: 10.1007/BF00413349.

Nurfiani, D., Wang, X., Gunawan, H., Triastuty, H., Hidayat, D., Wei, S. J., Taisne, B., Bouvet de Maisonneuve, C. (2021). Combining petrology and seismology to unravel the plumbing system of a typical arc volcano: An example from Marapi, West Sumatra, Indonesia. Geochemistry, Geophysics, Geosystems, 22, e2020GC009524. doi: 10.1029/2020GC009524.

Pratama, A., Bijaksana, S., Abdurrachman, M., Santoso, N.A. (2018): Rock Magnetic, Petrography, and Geochemistry Studies of Lava at the Ijen Volcanic Complex (IVC), Banyuwangi, East Java, Indonesia. Geosciences, 8, 183. doi:10.3390/geosciences8050183.

Peccerillo, A., Taylor, S.R. (1976): Geochemistry of Eocene Calc-Alkaline Volcanic Rocks from the Kastamonu Area, Northern Turkey. Contribution on Mineralogy and Petrology, 58, 63-81. doi: 10.1007/BF00384745.

Purbo-Hadiwidjojo, M. M., Samodra, I. L., dan Amin, T. C. (1998): Peta Geologi Lembar Bali, Nusa Tenggara Edisi Kedua, Pusat Penelitian dan Pengembangan Geologi.

Purnomo, B. J., Pichler, T. (2015): Geothermal systems on the island of Bali, Indonesia. Journal of Volcanology and Geothermal Research, 304, 349–358. doi: 10.1016/j.jvolgeores.2015.09.016.

Renjith, M.L. (2014): Micro-textures in plagioclase from 1994-1995 eruption, Barren Island. Geoscience Frontiers, 5, 113-126. doi: 10.1016/j.gsf.2013.03.006.

Reubi, O., Nicholls, I. A. (2004): Magmatic evolution at Batur volcanic field, Bali, Indonesia: petrological evidence for polybaric fractional crystallization and implications for caldera-forming eruptions. Journal Volcanology and Geothermal Research, 138, 345–369. doi: 10.1016/j.jvolgeores.2004.07.009.

Reubi, O., Nicholls, I. A. (2005): Structure and Dynamics of a Silicic Magmatic System Associated with Caldera – Forming Eruptions at Batur Volcanic Field, Bali, Indonesia. Journal Petrology, 46, 1367-1391. doi:10.1093/petrology/egi019.

Sahoo, S., Tiwari, D. K., Panda, D., Kundu, B. (2022): Eruption cycles of Mount Etna triggered by seasonal climatic rainfall, Journal of Geodynamics, 149, 101896. doi: 10.1016/j.jog.2021.101896.

Santoso, N.A., Bijaksana, S., Kodama, K., Santoso, D., Dahrin, D. (2017): Multimethod approach to the study of recent volcanic ashes from Tengger Volcanic Complex, Eastern Java, Indonesia. Geosciences, 7, 63. doi: 10.3390/geosciences7030063.

Sukmantara, G. D., Arthana, I. W., Kartika, G. R. A. (2021): Performance of Milkfish (Chanos chanos) Cultured by Different Stocking Density in Floating Net Cages Lake Batur, Trunyan Village, Bali. Advances in Tropical Biodiversity and Environmental Sciences 5(1), 29-33. doi: 10.24843/ATBES.v05.i01.p05.

Sutawidjaja, S.I., Chaniago, R., Kamal S. (1992): Geological Map of Batur Caldera, Bali, Indonesia. Indonesian Volcanological Directorate.

Syahbana, D. K., Kasbani, K., Suantika, G., Prambada, O., Andreas, A. S., Saing, U. B., Kunrat, S. L., Andreastuti, S., Martanto, M., Kriswati, E., Suparman, Y., Humaida, H., Ogburn, S., Kelly, P. J., Wellik, J., Wright, H. M. N., Pesicek, J. D., Wessels, R., Kern, C., Lisowski, M., Diefenbach, A., Poland, M., Beauducel, F., Pallister, J., Vaughan, R. G., Lowenstern, J. B. (2019): The 2017–19 activity at Mount Agung in Bali (Indonesia): intense unrest, monitoring, crisis response, evacuation, and eruption. Science Report, 9, 8848. doi: 10.1038/s41598-019-45295-9.

Wang, D.; and Van der Voo, R. (2004): The hysteresis properties of multidomain magnetite and titanomagnetite/titanomaghemite in mid-ocean ridge basalts. Earth and Planetary Science Letters, 220, 175-184. doi: 10.1016/S0012-821X(04)00052-4.

Wheller, G.E., Varne, R. (1986): Genesis of dacitic magmatism at Batur Volcano, Bali, Indonesia: implication for the origins of stratovolcano calderas, Journal Volcanology and Geothermal Research. 28, 363– 378. doi: 10.1016/0377-0273(86)90031-4.

Zhou, W., Van der Voo, R., Peacor, D. R., Zhang, Y. (2000): Variable Ti-content and grain size of titanomagnetite as a function of cooling rate in very young MORB. Earth and Planetary Science Letters, 179, 9 – 20.

SAŽETAK

Preliminarna petromagnetska istraživanja lava iz 1849., 1926., 1963., 1968. i 1974. godine iz vulkana Batur, Bali, Indonezija: uvid u magmatski proces izvora i magnetsku prirodu stijena

Geokemijska i petrografska istraživanja provedena na pet epizodnih efuzivnih erupcija iz vulkana Batur na otoku Baliju, Indonezija, otkrila su kako su te lave bazaltnoga do andezitskoga sastava. Prepoznate su različite mikroteksture odražavajući magmatske procese koji su prethodili erupcijama, kao i miješanje magme te adijabatska dekompresija. Načinjene su XRF analize, uz koje su pet tokova lave (L849, L926, L963, L968 i L974) također ispitani magnetskim analizama mjerenja magnetske susceptibilnosti i histereze. Na cikličnost magmatskoga procesa upućuju varijacije vrsta mikrotekstura, sadržaja CaO i vrijednosti magnetske susceptibilnosti. Prikazana su dva moguća modela navedene cikličnosti. U prvome modelu cikličnost je prouzročena varijacijom dotoka iz donje komore magme, što je utjecalo na njezino međudjelovanje s okolnim stijenama. U drugome modelu na cikličnost utječe pojava novoga magmatskog toka koji ima snažno međudjelovanje s okolnim stijenama. Studija upućuje na to da zajedničko korištenje analize mikrotekstura, sastava i magnetske susceptibilnosti može dati uvid u cikličnost epizoda istjecanja lave opaženih u aktivnim vulkanima kao što je Batur.

Ključne riječi:
vulkan Batur, magmatizam, magnetizam stijena, Bali

Author's contribution

Putu Billy Suryanata (1) (M.Eng., Geophysical Engineering with expertise in rock magnetism for volcanoes) performed the field work and rock sample data collection, magnetic data measurements and processing, provided the data interpretation, composed the original draft, edited and performed project administration. **Satria Bijaksana (2)** (Ph.D., Professor, expert on rock magnetism) provided the rock magnetism data interpretation, edited the draft, held funding acquisition, supervision, and project administration. **Mirzam Abdurrachman (3)** (Ph.D., Associate Professor, expert on petrogeology in volcanic area) provided the petrography and geochemical interpretation, edited the draft and supervised. **Darharta Dahrin (4)** (Ph.D., Associate Professor, expert on statistical analysis and geomagnetic) provided the rock magnetism and statistical analysis data interpretation, performed proofreading and supervision. **Aditya Pratama (5)** (Ph.D., Researcher, expert on in rock magnetism and petrography for volcanoes) performed magnetic data measurements, provided rock magnetic, petrography and geochemical data interpretation and proofreading. **Nuresi Rantri Desi Wulan Ndari (6)** (M.Eng., Geophysical Engineering with expertise on rock magnetism) performed the field work and rock sample data collection, interpretation in rock magnetic data and proofreading. **Silvia Jannatul Fajar (7)** (M.Eng. Assistant Professor, expert on rock magnetism for lakes) performed magnetic data measurements, provided rock magnetic data interpretation and proofreading.